Effect of Ball Diameter on Mechanical Alloying Process for the Production of Dispersion Strengthened Tungsten

Hiroyuki NOTO,　Yoshimitsu HISHINUMA and　Takeo MUROGA

National Institute for Fusion Science, Toki, Gifu 509-5292, Japan

Tungsten is candidate material for plasma facing armor. In our initial study, to improve the plasma facing tungsten on fusion divertor, a new oxide dispersion strengthened tungsten (ODS-W) has been developed using by REDOX (oxidation-reduction reaction) process between W and TiC, including titanium oxide as strengthening nano-particles in matrix, fabricated by mechanical alloying (MA)-hot isostatic pressing (HIP), which can inhibit the decrease of mechanical property even after recrystallization occurs. Our past studies showed that the condition of MA process affects the mechanical and the thermal properties of the products. In the present study, the optimal ball size to be used in the MA process of preparing ODS-W has been proposed by investigation of the relationship between different ball sizes and the MA effect, focusing the optimization of manufacturing process for DS-W. The evolutions of the lattice constant and microstructure were shown to indicate the progress of mechanical alloying. The effect of the ball size was interpreted as that of collision energy delivered by the weight of MA balls.

© 2024 The Japan Society of Plasma Science and Nuclear Fusion Research

1. Introduction

Tungsten (W) has been considered as plasma facing material (PFM) on heat removal component of a divertor. The heat load on surface of PFM is becoming increasingly severe with enhancing plasma condition [1]. Accordingly, tungsten materials for PFM are required as heat resistant which can inhibit the thermal change of its component during operation. To satisfy the requirement, varied high performance tungsten materials have been developed in previous studies. The candidate tungsten materials can be classified as follows: (1) tungsten-rhenium alloy strengthened by solid solution [2], (2) composite reinforced tungsten [3], (3) coating tungsten such as chemical vapor deposition (CVD) or physical vapor deposition (PVD) [4], (4) potassium doped tungsten strengthened by nano-bubbles [5], (5) dispersion strengthening tungsten (DS-W) strengthened by nano-compound particles in matrix [6], and others (In this paper, dispersion strengthened tungsten was defined as DS-W). However, the tungsten matrix has critical issue of recrystallization induced embrittlement because the grain boundaries are weakened after the recrystallization. For the solution of the problem, the suppression of embrittlement by the increase of recrystallization temperature have been tried in studies of (1) and (4). On the other hand, there is a materials design which can avoid embrittlement even after recrystallization on DS-W (5) including the effects of grains pinning [7] or grain boundary strengthening [8, 9]. Regarding the previous studies about DS-W

strengthening nano-particles in matrix, the DS-W can be classified in term of kind of the nano-particle in matrix as follows, W- lanthanum (La) compound [10], W- yttrium (Y) compound [11], Y-titanium (Ti) composite compound [12], TiO_2 applied REDOX (oxidation-reduction reaction) effect between TiC and impurity in our previous study [13], TiC [14]. Considering the requirement for high performance of tungsten in the future, further improvement by new strengthening nano-particles in matrix is expected. For the fabrication of DS-W, generally, mechanical alloying (MA) is known as essential process, important in view of material design on DS alloys, which is generally reached to the metastable-forced solid solution state by continues folding of particles of MA powders with collision between the powders. Although establishing the MA process needs evaluation of alloyed state as shown in previous studies of other DS alloys [15–17], detail research of alloying process on DS-W has not been studied. Therefore, it is expected that this study provides the necessary data for upgrading the performance of advanced DS-W. The previous study showed the effect of ball diameter on the collision energy [18, 19]. The results indicated that the difference of ball diameter directly affected that of the collision energy which is associated with the MA progression. In addition, MA progression data every base material is needed because the progression rate also differ in case of different base material. In this paper, the effect of ball diameter on the micro-structure of particles of MA powders and the crystal structure in MA process is elucidated based on our research of DS-W including nano-oxide titanium particles

_____

author's e-mail: noto.hiroyuki@nifs.ac.jp

Table 1 Data of raw powders.

Materials	Purity (%)	Particle size (μm)
Tungsten	99.95	1.0
Titanium Carbide	98.00	1.8

in matrix.

2. Experimental Procedure

In the preparation of alloying for DS-W alloys, the initial materials used were powders of pure-tungsten and titanium carbide supplied by New Metals and Chemicals Co. LTD. and JAPAN NEW METALS Co. LTD., respectively. The data of the powders supplied by the vendors are listed in Table 1. The initial materials were mixed and mechanically alloyed in a planetary-type ball mill made by Fritsch Co.,Ltd using tungsten carbide MA balls of 1.6 mm.3.0 mm and 5.0 mm in a 250 cc tungsten carbide MA pot with ball-powder ratio of 2:1. The alloying was carried out with a rotating rate of 360 rpm for 64 hrs in a purified argon gas atmosphere with an oxygen concentration of less than 1 ppm. The rotation was repeated by an automated program (20 min milling + 3 hr pause) to avoid excess temperature increase of the pot, and the alloying time of 64 hrs was the total of the milling time, not included pause time. The transition of sectional microstructure on the mechanical alloyed powders was observed by using the focused ion beam (FIB) -scanning electron microscopy (SEM). The lattice constant (LC) for evaluation of the metastable solid-solution state between matrix and compound and the full width at half maximum (FWHM) for evaluation of the strain were characterized by $2\theta/\theta$ method and θ method, respectively. The FWHM is broad width of the peak on half of the peak height.

3. Results and Discussion

Figure 1 (a) shows XRD diffraction patterns of the powders after 0, 4,64 hr MA with 1.6, 3.0, 5.0 mm ball and the pure tungsten. The peak exhibited the shift to low angle, the broad with the MA time finally, which means the lattice dilatation and amorphization, respectively on tungsten matrix. Figure 2 shows LC and FWHM of tungsten matrix with MA time, indicating the lattice dilatation of tungsten matrix and the inner strain accumulation of MA powders, respectively. The lattice constants was derived by Bragg's law (1)

$$n\lambda = 2d \sin\theta. \tag{1}$$

λ,d and θ is wave length, lattice constant and glancing angle, respectively. According to Fig. 1 (b) showing lattice constants, MA powders with 1.6, 3.0 and 5.0 mm balls exhibited a rise and fall of the lattice constant from 0 hr MA

to 8 hr MA slightly, then, started the re-dilatation from 8 hr MA to 16 hr MA. The slight change of lattice constant indicates that MA less than 16 hr is not sufficient for alloying, and formed inhomogeneous micro-structure. The lattice constant of the MA powder with 1.6 mm ball after 64 hr MA time did not reach that of pure tungsten, inferring that the forced solid-solution state did not occur between tungsten matrix and titanium element. On the other hand, lattice constants of MA powders with 5.0 and 3.0 mm balls exceeded that of pure tungsten from 16 hr to 32 hr, implicating the starting of mechanical alloying between tungsten matrix and titanium element. Finally, both MA powders with 3.0 and 5.0 mm ball exhibited the dilatations of 0.14 % and 0.29 % after 64 hr MA. According to Fig. 1 (c) showing Full Width at Half Maximum with MA time, MA powders with 1.6, 3.0 and 5.0 mm balls exhibited that the FWHM re-increased after once stop of increasing FWHM. On the plot of MA powder with 3.0 and 5.0 mm ball, the stop and the re-increase of FWHM occurred when each FWHM exceeds the FWHM of pure tungsten. Therefore, considering these trends, it is expected that the FWHM increased after 64 hr MA in case of MA with 1.6 mm ball.

Figures 2 (a) (b) shows the surface shape of powders before and after MA. Although the surface of initial tungsten powders has sharp corners in the start of MA, the powders was gradually rounded off the surface corner, finally changed to refine powders with MA proceeding. Figure 2 (c) shows the cross section of MA powders with the MA time, which visibly exhibits the needed lamination state of nano-order in production process of ODS alloy.

In this result, the phases reached to laminated state, and it was defined in following. (1.agglomeration: Start of joints between powders, 2.adhesion: compacted state more than agglomeration, 3.formation of membrane: formation of a layer in the powder surface, 4.Swelling membrane: the membrane changes to thickly, 5.Partial lamination: formation of several coating, 6.all lamination: powder-wide lamination).The agglomeration of MA powders with 1.6 mm ball started at 4 hr MA, then, changed to the adhesion shape seeming the packed powders. After 16 hr MA, the membrane shape on surface of the powder formed followed by the adhesion shape, and changed to the swelled shape after 32 hr MA. MA powder of final phase on 64 hr MA with 1.6 mm ball formed the partial lamination shape such as pile-upped the membrane shape. The partial lamination shape on MA powder with 3.0 mm ball was observed after 16 hr MA, then, changed to all lamination shape, and changed to homogenized shape after 64 hr MA finally. The difference of the transition on MA with 1.6 and 3.0 mm ball implied that 64 hr MA with 1.6 mm ball is not sufficient. On the other hand, the partial lamination shape on MA powder with 5.0 mm ball started from 8 hr MA with restrained void in powder, finally reached the homogenized shape after 32 hr, following all lamination shape at 16 hr MA. Considering these results of the microstructure, the FWHM and the lattice constant on MA powders, "once
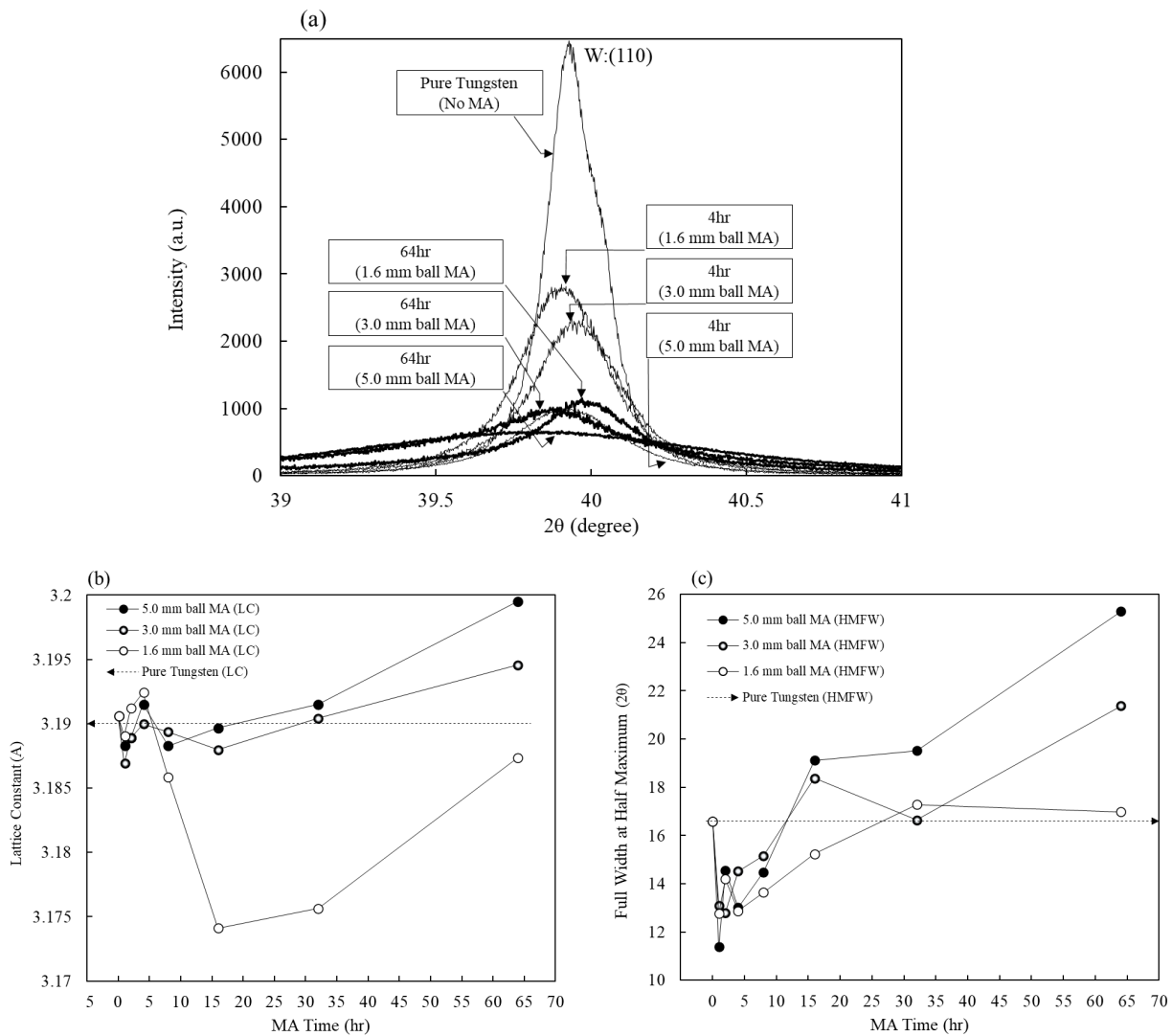
Fig. 1   Lattice constant and Full Width at Half Maximum with MA time. (a) XRD diffraction patterns of the powders after 0, 4, 64 hr MA with 1.6, 3.0, 5.0 mm ball, (b) Lattice constant, (c) Full Width at Half Maximum.

stop and re-increase" of the increasing FWHM occurred when the lattice dilatation beyond the pure tungsten. In addition, it appeared that the microstructure changed from partial lamination to all lamination at that time, implying that the formation of lamination microstructure affected the starting of lattice dilation. Thus, it is predicted that MA with 1.6 mm ball would exhibit the above mentioned lattice dilatation and re-increase of FWHM after 64 hr MA.

The MA time needed to lattice dilatation in case of MA with 1.6 mm ball and the ball diameter needed for the lattice dilatation in 64 hr MA were predicted in term of lattice dilatation. Figure 3 (a) shows lattice constant of 1.6 mm ball MA which reached the lattice dilatation at 64 hr. Considering the fitted MA curve after 16 hr (2), it is predicted that lattice dilatation of 1.6 mm ball MA reaches after 72.2 hr.

$$y = 3.1683e^{9E-5x}. \tag{2}$$

Figure 3 (b) shows rates of lattice dilatation with ball

diameter after 64 hr MA. These rates of lattice dilatation was drawn as exponential curve (3).

$$y = 0.3348\ln(x) - 0.2349. \tag{3}$$

Even though lattice constant of MA powder with 1.6 mm ball did not approach that of pure tungsten after 64 hr MA, both MA powders with 3.0 and 5.0 mm ball exhibited the dilatations of 0.14 % and 0.29 %, relatively, relative to lattice constant of pure tungsten. According to the fitted curve, it was derived that ball diameter more than 2.0 mm is required for reach to the lattice dilatation at 64 hr MA. The MA by using balls more than 2.0 mm in diameter will complete the alloying in 64 hr, indicating the potential contribution to efficient shortening of total MA time for the future studies of DS-W. On the other hand, use of balls more than 5.0 mm in diameter is not adequate because of risk of inducing fracture of pot by high collision energy. Thus, considering the exponential curve, it would
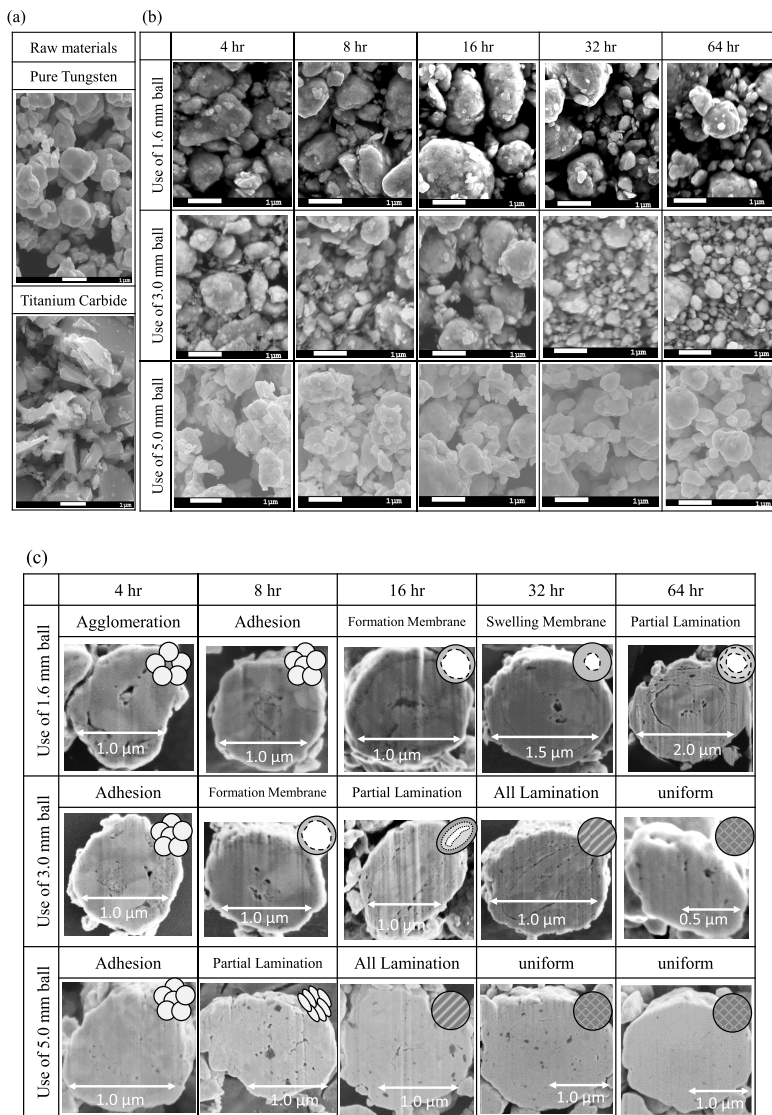
Fig. 2   Raw materials and MA powders. (a) Powder shape of Raw Materials, (b) Surface of MA powder by the MA time, (c) Cross section of MA powder by the MA time.
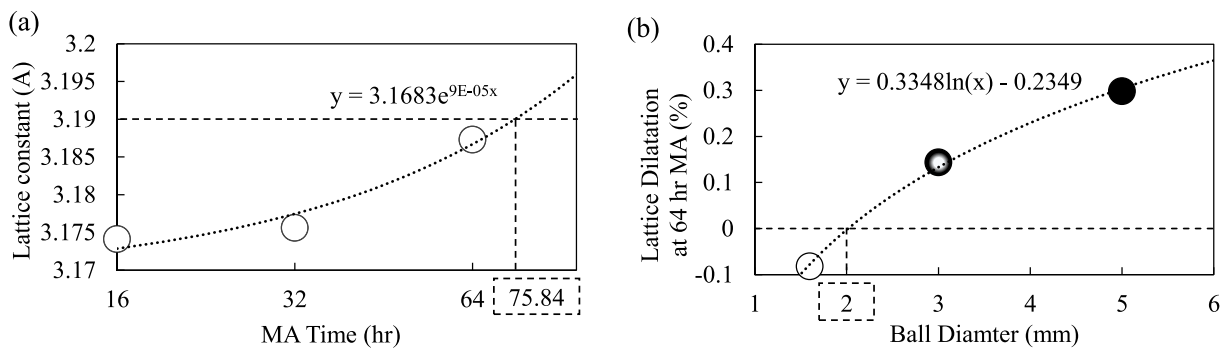
Fig. 3   Predictions of the necessary MA time and ball diameter for lattice dilatation. (a) Lattice constant of MA powder with 1.6 mm balls from 16 hr to 64 hr, (b) Lattice dilatation of MA powder by use of different MA ball at 64 hr MA.

be judged that use of balls from 2.0 mm diameter to 5.0 mm diameter is adequate. In addition, above relationship discussion between the ball size correlating the shortage of manufacturing process and the lattice dilatation indicating start of forced solid solution will also contribute to for future process of manufacturing ODS-W.

4. Conclusions

For the production of dispersion strengthening tungsten (DS-W), Mechanical Alloying (MA) is an essential process. In this study, the steps by mechanical alloyed state were researched in views of the micro-structure and the crystal structure. The main results are as follows:

1. The lattice constants of MA powders with 5.0 and 3.0 mm balls exceeded that of pure tungsten from 16 hr to 32 hr, implicating the starting of mechanical alloying between matrix and additional element. The results of lattice constant of FWHM indicated that 64 hr MA with 1.6 mm ball is not sufficient for alloying.

2. Based on the result of insufficient MA with 1.6 mm ball and that of sufficient MA with 3.0 to 5.0 mm ball, it is interpreted that the cross sectional microstructure in the powders with MA time transited in the following order: agglomeration of particles, adhesion of particles, formation of membrane, partial lamination to all lamination and finally homogenization.

3. Considering the result of crystal structure analysis and that of cross sectional observation on the MA particles, these results showed that a behavior of the increasing FWHM, when lattice dilatation occurred beyond the lattice constant of pure tungsten, appeared with microstructure transition from the partial lamination to the all lamination.

4. The factor such as MA time and MA ball diameter correlated with the lattice dilatation associating the progress in alloying. The plot of lattice dilatation between MA time and MA ball diameter was shown as exponential relation, which was derived by the necessary time and the ball diameter for alloying. The results indicates the possibility of shortening of total MA time by effective introduction of strain during MA.

[1] M. Tokitani *et al.*, Advanced multi-step brazing for fabrication of a divertor heat removal component, Nucl. Fusion **61**, 046016 (2021).

[2] M. Fukuda *et al.*, Microstructural development of tungsten and tungsten–rhenium alloys due to neutron irradiation in HFIR, J. Nucl. Mater. **455**, 460 (2014).

[3] J. Reiser *et al.*, Tungsten foil laminate for structural divertor applications, J. Nucl. Mater. **423**, 1 (2012).

[4] G.-N. Luo, Q. Li *et al.*, Coating materials for fusion application in China, J. Nucl. Mater. **417**, 1257 (2011).

[5] S. Nogami *et al.*, Effect of microstructural anisotropy on the mechanical properties of K-doped tungsten rods for plasma facing components, Fusion Eng. Des. **109-111**, 1549 (2016).

[6] M. Fukuda *et al.*, Microstructure development of dispersion-strengthened tungsten due to neutron irradiation, J. Nucl. Mater. **449**, 213 (2014).

[7] H. Noto *et al.*, Thermal change of microstructure and mechanical properties of dispersion strengthened tungsten, Nucl. Fusion **61**, 116001 (2021).

[8] H. Kurishita *et al.*, Development of Nanostructured Tungsten Based Materials Resistant to Recrystallization and/or Radiation Induced Embrittlement, Mater. Trans. **54**, 456 (2013).

[9] H. Kurishita *et al.*, Development of ultra-fine grained W–TiC and their mechanical properties for fusion applications, J. Nucl. Mater. **367-370**, 1453 (2007).

[10] M. Rieth *et al.*, Limitations of W and W–1%La$_2$O$_3$ for use as structural materials, J. Nucl. Mater. **342**, 20 (2005).

[11] G. Yao *et al.*, Excellent performance of W–Y$_2$O$_3$ composite via powder process improvement and Y2O3 refinement, Mater. Des. **212**, 110249 (2021).

[12] M.V. Aguirre *et al.*, Mechanical properties of tungsten alloys with Y$_2$O$_3$ and titanium additions, J. Nucl. Mater. **417**, 516 (2011).

[13] H. Noto *et al.*, Formation Mechanism of Nano-Strengthening Particles in Dispersion Strengthened W-Ti Alloys, Plasma Fusion Res. **15**, 1205021 (2020).

[14] H. Kurishita *et al.*, Development of re-crystallized W–1.1%TiC with enhanced room-temperature ductility and radiation performance, J. Nucl. Mater. **398**, 87 (2010).

[15] M. Yamamoto *et al.*, Reverse phase transformation from α to γ in 9Cr-ODS ferritic steels, J. Nucl. Mater. **417**, 237 (2011).

[16] B. Ma *et al.*, Development of Y2O3 dispersion strengthened Cu alloy using Cu6Y and Cu2O addition through the MA-HIP process, Fusion Eng. Des. **161**, 112045 (2020).

[17] Q. Tang *et al.*, Refinement of Oxide Particles by Addition of Hf in Ni-0.5 mass%Al-1 mass%Y$_2$O$_3$ Alloys, Mater. Trans. **51**, 2019 (2010).

[18] T.H. Courtney *et al.*, Process Modeling of Mechanical Alloying, Mater. Trans. **36**, 110 (1995).

[19] G.B. Schaffer *et al.*, The influence of collision energy and strain accumulation on the kinetics of mechanical alloying, J. Mater. Sci. **32**, 3157 (1997).